bioRχiv

Brightness illusions evoke pupil constriction and a visual cortex response in rats

Dmitrii Vasilev[a,b,c], Isabel Raposo[c], and Nelson K. Totah[a,b,c,*]
[a]Helsinki Institute of Life Science (HILIFE), University of Helsinki, 00014 Helsinki, Finland
[b]Faculty of Pharmacy, University of Helsinki, 00014 Helsinki, Finland
[c]Max Planck Institute for Biological Cybernetics, 72076 Tuebingen, Germany
*Correspondence should be addressed to N.K.T. (nelson.totah@helsinki.fi)

Luminance causes the pupillary light response (PLR), a constriction of the pupil. Surprisingly, mere illusions of brightness evoke a pupil constriction in humans. Since brightness illusions depend on scene and context, this suggests that high-level visual processing has a top-down influence onto the brainstem neurons controlling the PLR. The influence of high-level vision on this brainstem-mediated reflex is thought to be restricted to primates that perform foveal fixation. Here, we report that the same brightness illusions that evoke a pupil constriction in humans also do so in rats (N = 14). This response occurred only for stimuli that matched the spectral sensitivity of the rat retina. We recorded 32-channel cortex-wide EEG and found that illusory brightness stimuli also evoked a larger primary visual cortex event-related potential. This neural response preceded pupil constriction by ~335 msec. Thus, primary visual cortex may contribute to the PLR evoked by passive viewing of brightness illusions. Our results resolve whether this phenomenon is confined to primates by showing that it can also be found in rats.

Introduction

The pupillary light response (PLR) is a reflex controlled by retinal ganglion cells activating a two-synapse brainstem circuit [1]. In humans, this automatic constriction to light is also engaged in response to mere illusions of brightness [2]. Visual illusions are thought to occur because visual cortex neurons do not simply respond to physical luminance on the retina, but instead respond based on contextual cues that were learned, either through early life experience or evolution of the species, to enable a heuristic approach to vision [3]. Thus, the gestalt of an image arising from high-level visual processing modulates this simple reflex controlled by the brainstem.

High-level visual perception involves multiple cortical regions, including primary and secondary visual cortex neurons, which respond to illusory brightness in non-human primates and in mice [4–6]. It is therefore likely that the visual cortex influences brainstem control over the pupil via still uncharted neuronal interactions. Rodents can provide a powerful means for studying these forebrain-brainstem interactions. However, it is currently unknown whether the influence of high-level vision on the pupil is confined to primates which use foveal vision or if it is present in animals without a fovea that preceded the evolution of primates [7].

In this study, we presented a brightness illusion to head-fixed rats. We used the "Asahi" stimulus, which was created by Prof. Akiyoshi Kitaoka (Department of Psychology, Ritsumeikan University, Osaka, Japan) based on luminance-gradient stimuli in earlier work [8]. Humans report perceiving a glare at the center of the Asahi stimulus, and it evokes a pupil constriction in humans [2] but it is unknown whether the same occurs in animals. Here, we show that the Asahi stimulus drives a pupil constriction in rats. On the other hand, a luminance-matched control stimulus, which does not evoke illusory brightness in humans, did not cause a pupil constriction in rats. The Asahi stimulus also drove a larger visual cortex EEG event-related potential. Our results show that the influence of high-level visual perception on the brainstem-controlled PLR reflex is not confined to foveating primates and that the rat is a viable animal model for studying the underlying neurophysiology of this phenomenon.

Results

Fourteen, male lister-hooded rats were head-fixed on a non-motorized treadmill and passively exposed to visual stimuli. Rats were free to walk or sit immobile during the experiment. We presented the Asahi stimulus (**Figure 1**), which humans perceive to have a bright glare in the center [2]. We

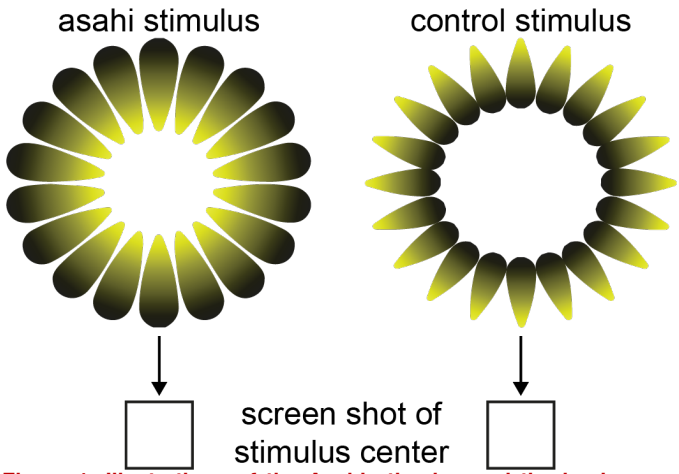

Figure 1: Illustrations of the Asahi stimulus and the luminance-matched control stimulus. The Asahi stimulus is typically perceived by humans to have a brighter-than-white glare in the center. By rearranging the stimulus to have a different shape, this brightness illusion is abolished. The screen shots show that the actual luminance at the center of each stimulus is identical, despite appearing to be brighter in the center of the Asahi stimulus.

also presented a luminance-matched control stimulus that due to rearrangement of the Asahi stimulus into a new structure, does not evoke a brightness percept in humans [2]. Although yellow stimuli (~580 nm wavelength) were used in the human study [2], the spectral sensitivity of the rat retina is diminished around 580 nm and lacking sensitivity over 590 nm, while it is very sensitive below 530 nm [9]. Therefore, in addition to presenting the yellow stimuli from prior work in humans, we also presented 508 nm (green) stimuli (**Supplementary Figure 1**). The stimuli were various sizes (10º, 20º, 40º, and 60º) and presented by tiling the entire visual field with as many stimuli as possible. An example of the 10º yellow Asahi stimulus and luminance-matched control stimulus are shown in **Supplementary Figure 2** and **Supplementary Figure 3**, respectively.

Pupil size was measured using video frames collected at 45 frames per sec. Environmental illumination was held constant throughout the experiment and across subjects by collecting the data in closed faraday cages with total darkness except for the stimulus screen. Each stimulus was presented 50 times in randomized order for 4 sec with a 4 to 8 sec inter-stimulus interval drawn from a distribution with a flat hazard rate. Between stimuli, we presented a grey screen that was equiluminant with the stimuli (15 lux measured at the head of the rat). The inter-stimulus intervals allowed ample time for the pupil to return to baseline and the flat hazard rate reduced expectation of stimulus onset.

The Asahi illusion evokes a pupil constriction in rats

Given the spectral sensitivity of the rat retina, we tested the hypothesis that the green Asahi illusion, but not the yellow version, would cause a pupil constriction in rats relative to the luminance-matched control stimulus. Since stimulus onset time was difficult to predict, we expected to observe a dilation of the pupil [10–12]. However, this dilation may be counteracted by competitive drive from parasympathetic activation of the sphincter pupillae muscle.

We observed a constriction of the pupil after onset of the 10º and 20º, green Asahi stimuli (**Figure 2**). The magnitude of constriction was larger for the Asahi stimulus compared to the control stimulus in those stimulus conditions. A Bayesian one-tailed t-test of the hypothesis that the

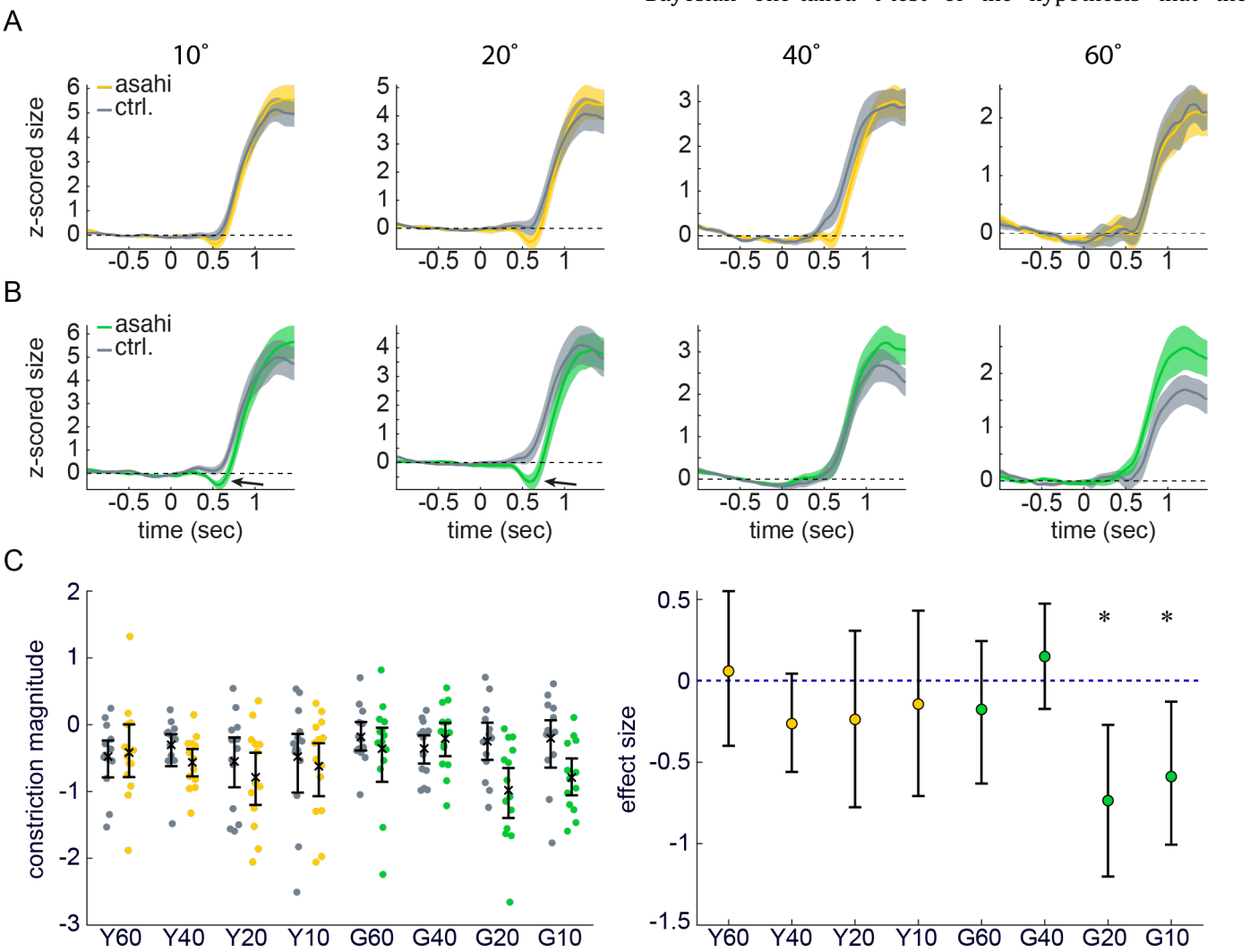

Figure 2: The Asahi stimulus evokes a pupil constriction in rats. (A, B) The SEM of pupil size is plotted from 1 sec before stimulus onset until stimulus offset at 4 sec later. Pupil size was normalized relative to the pre-stimulus pupil size using a z-score. The grey line is the pupil size around the control stimulus and the colored line is relative to the Asahi stimulus. Panel A shows the pupil response to yellow stimuli and panel B shows the response to green stimuli. A constriction relative to baseline is apparent for 10° and 20° green stimuli (arrows). **(C)** The minimal pupil size (z-scored) in the first 750 msec after stimulus onset is plotted for each stimulus. Dots are individual rats. In the yellow 60°, 40°, and 20° conditions and the green 10° condition, only 13 rats are plotted due to data loss. The right panel shows the effect size between the Asahi stimulus and the control stimulus. The asterisks indicate support for the alternative hypothesis ($BF_{10} > 3$).

magnitude of constriction was larger for the Asahi stimulus was strongly supported by these data (green, 20º stimuli: BF_{10} = 14.68; green, 10º stimuli: BF_{10} = 6.36). The SEM of the constriction latency was 578.6±67.6 msec for the green 10º Asahi stimulus and 575.4±61.8 msec for the green 20º Asahi stimulus.

We consider it unlikely that fixation on local changes in contrast could explain the observed pupil constriction. Fixation on local contrast changes is improbable because rats do not have foveal vision [13] and the visual acuity of rats is lower than sharp changes in local contrast of the 10º and 20º stimuli [14,15]. Moreover, the same black-to-white contrast changes occur in the yellow and green stimuli, yet only the green Asahi stimuli were associated with a pupil constriction. However, we additionally compared eye position found that they did not differ between the two stimuli during the first 600 msec after stimulus onset, which was the window during which the pupil constriction was observed. Bayesian paired t-tests comparing the location of the center of the pupil between the green Asahi stimulus and green luminance-matched control stimulus supported the null hypothesis that location did not differ (x-position for 20º and 10º stimuli were BF_{10} = 0.34 and BF_{10} = 0.34, respectively; y-position for 20º and 10º stimuli were BF_{10} = 0.29 and BF_{10} = 0.34, respectively). Moreover, saccades were rare and saccade rate did not differ between stimulus conditions. The 20º and 10º Asahi stimuli had saccade rates of 0.597±0.062 and 0.859±0.083, whereas the 20º and 10º luminance-matched control stimuli had saccade rates of 0.602±0.060 and 0.834±0.079 (SEM). The observed saccade rates strongly supported the null hypothesis that mean saccade rate was similar for the Asahi stimulus and the luminance-matched control stimulus for both the 20º stimuli or the 10º stimuli (BF_{10} = 0.15 and 0.12, respectively).

The visual cortex responds to the Asahi stimulus in rats

We next assessed whether the Asahi stimulus differentially engaged visual cortex in comparison to the luminance-matched control stimulus. If high-level visual processing differences contribute to perception of the brightness illusion in humans, then the Asahi stimulus may also be associated with different visual cortex activity. In 10 of the 14 rats, we recorded EEG from most of the cortex using a 32-electrode array implanted directly onto the skull and aligned to bregma. Twelve electrodes covered bilateral primary and secondary visual cortex. We obtained event-related potentials (ERPs) for each electrode in a window starting 750 msec before stimulus onset and lasting until 750 msec after stimulus onset, and then plotted the maximal ERPs across all visual cortex electrodes. The Asahi and the control stimuli evoked a response for both yellow and green stimuli of all sizes (**Supplementary Figure 4A,4B**). A Bayesian one-sided t-test of the hypothesis that the ERP peak was larger for the "brighter" stimulus (i.e., the Asahi stimulus) in comparison to the control stimulus was supported in the case of the 10º green Asahi stimulus (BF_{10} = 5.67, **Figure 3A, 3B**). Notably, this Asahi stimulus also evoked a pupil constriction. The SEM of the ERP peak latency after stimulus onset was 244.1±8.0 msec for the green 10º Asahi stimulus. A topographical plot of the ERP peak magnitude shows that it was confined to visual cortex for the Asahi and the control stimuli (**Figure 3C**). These electrodes were located at 5.0 mm and 7.0 mm posterior to bregma with 3 electrodes (per hemisphere) at each posterior location situated laterally from bregma at 1.5 mm (overlaying V2MM), 3.0 mm (overlaying V2ML at the anterior electrode and V1M at the posterior electrode), and 4.4 mm (overlaying V1 at the anterior electrode and V1B at the posterior electrode). The ERP was largest over V1.

Discussion

Illusions are a powerful tool for studying how the brain constructs visual scene using contextual cues [16]. Human interpretation of scene and context activates the reflexive pupillary constriction to changes in luminance [2,17]. The neuronal connections that allow high-level image content to influence this brainstem-mediated reflex are unknown and would benefit from a rodent model that permits probing cell types and specific neuronal projections using single cell recordings and optogenetic tagging of neurons by their projection target. However, it is debated whether this capacity for brightness illusions to evoke pupil constriction evolved in primates or if it also evolved in early mammals. Here, using a novel combination of head-fixation, pupillometry and EEG recordings in rats, we show that the pupil constricts after the Asahi illusion and is associated with visual cortex neural activity. Therefore, top-down modulation of this reflex is not restricted to primates with foveal vision and might have already evolved in early mammals.

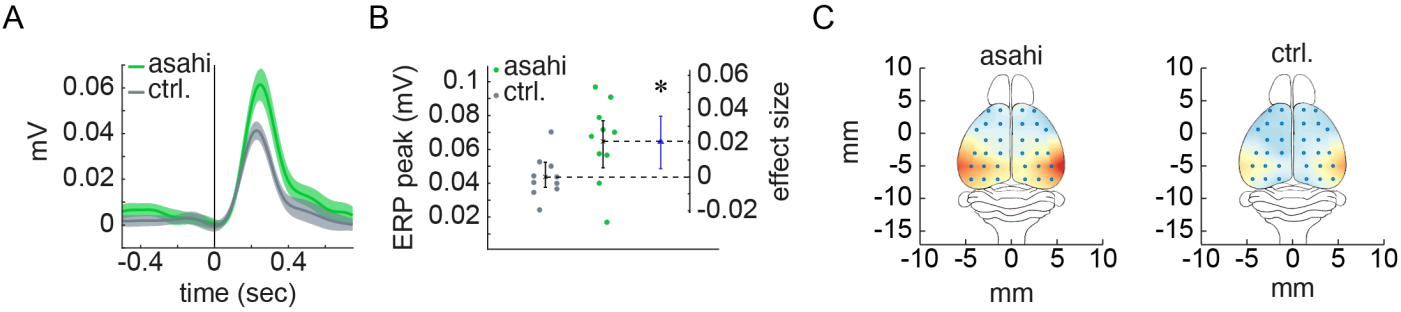

Figure 3: An Asahi stimulus that evoked pupil constriction also evoked a larger event-related potential in visual cortex. (A) The SEM of the visual cortex EEG is plotted from 750 msec before and until 750 msec after stimulus onset. The grey line is the ERP around the control stimulus and the colored line is relative to the green 10° Asahi stimulus. **(B)** The maximal potential in the ERP is plotted for each stimulus. Dots are individual rats. The inset shows the effect size between the Asahi stimulus and the control stimulus in mV. The asterisk indicates support for the alternative hypothesis (BF10 > 3). **(C)** The average ERP peak magnitude across 10 rats is shown on a scale of 0 mV (blue) to 0.06 mV (red). Electrode locations are shown relative to bregma at the origin.

Visual cortex neural activity related to scene processing may activate reflexive pupil constriction

Our findings are consistent with visual cortex neuronal activity, which is related to processing of the Asahi stimulus, driving a subsequent pupil constriction. We found that illusory brightness evoked a larger EEG ERP in visual cortex compared to a luminance-matched control stimulus. The latency of the maximal ERP after the 10º green Asahi stimulus was 244 msec and thus preceded the pupil constriction, which occurred at a latency of 579 msec.

The pupil constriction evoked 579 msec after the Asahi stimulus occurred later than the pupil response to an actual increase in luminance, which requires approximately 250 msec for high intensity light and as much as 400 msec for very low intensity light [18–20]. The PLR is mediated by only a few synapses: from retinal ganglion cells to the midbrain olivary pretectal nucleus and immediately to the preganglionic Edinger-Westphal nucleus that activates the ciliary ganglion of the parasympathetic nervous system [21,22]. This short pathway constitutes a simple reflex in response to changes in luminance. The constriction in response to the Asahi stimulus is greatly delayed in comparison to constrictions in response to luminance. Our finding supports the notion that additional synapses, presumably in the forebrain and involving visual cortex, intercede between the retina and the brainstem to evoke a pupil constriction due to illusory brightness.

Evidence for the innateness of high-level visual processing influences on brainstem-controlled pupil constriction

It has been debated whether the influence of high-level vision on the pupil is due to the early life experience of individuals or evolved across generations of individuals [7]. Recent evidence suggests that early life experience does not play a role in perceiving illusions based on visual scene and context [23]. In that study, 8- to 12-year-old children who recently gained depth perception were immediately susceptible to illusions related to depth perception. However, since the influence of high-level vision on pupil constriction has only been previously demonstrated in humans [2,17], it is an open question whether other mammals have this capability. Our findings in rats support the idea that neuronal processing of high-level visual content and its influence on the brainstem-mediated PLR reflex is present at an earlier stage than primates. Moreover, our results show that the rat is a viable model for studying the single neuron correlates of brightness illusions in the visual cortex and the neuronal connections via which high-level vision affects brainstem control of the pupil.

References

1. McDougal, D.H., and Gamlin, P.D. (2017). Comprehensive Physiology. Compr Physiol *5*, 439–473.
2. Laeng, B., and Endestad, T. (2012). Bright illusions reduce the eye's pupil. Proc National Acad Sci *109*, 2162–2167.
3. Purves, D., Williams, S.M., Nundy, S., and Lotto, R.B. (2004). Perceiving the Intensity of Light. Psychol Rev *111*, 142–158.
4. Pak, A., Ryu, E., Li, C., and Chubykin, A.A. (2019). Top-Down Feedback Controls the Cortical Representation of Illusory Contours in Mouse Primary Visual Cortex. J Neurosci *40*, 648–660.
5. Rossi, A.F., Rittenhouse, C.D., and Paradiso, M.A. (1996). The Representation of Brightness in Primary Visual Cortex. Science *273*, 1104–1107.
6. Roe, A.W., Lu, H.D., and Hung, C.P. (2005). Cortical processing of a brightness illusion. Proc National Acad Sci *102*, 3869–3874.
7. Binda, P., and Murray, S.O. (2015). Keeping a large-pupilled eye on high-level visual processing. Trends Cogn Sci *19*, 1–3.
8. Zavagno, D. (1997). Some New Luminance-Gradient Effects. Perception *28*, 835–838.
9. Peirson, S.N., Brown, L.A., Pothecary, C.A., Benson, L.A., and Fisk, A.S. (2018). Light and the laboratory mouse. J Neurosci Meth *300*.
10. Beatty, J. (1982). Phasic Not Tonic Pupillary Responses Vary With Auditory Vigilance Performance. Psychophysiology *19*, 167–172.
11. Breton-Provencher, V., and Sur, M. (2019). Active control of arousal by a locus coeruleus GABAergic circuit. Nat Neurosci *22*, 218–228.
12. Murphy, P.R., Robertson, I.H., Balsters, J.H., and O'connell, R.G. (2011). Pupillometry and P3 index the locus coeruleus-noradrenergic arousal function in humans. Psychophysiology *48*, 1532 1543.
13. Euler, T., and Wässle, H. (1995). Immunocytochemical identification of cone bipolar cells in the rat retina. J Comp Neurol *361*, 461–478.
14. Prusky, G.T., Harker, K.T., Douglas, R.M., and Whishaw, I.Q. (2002). Variation in visual acuity within pigmented, and between pigmented and albino rat strains. Behav Brain Res *136*, 339–348.
15. Artal, P., Tejada, P.H. de, Tedó, C.M., and Green, D.G. (1998). Retinal image quality in the rodent eye. Visual neuroscience *15*, 597 605.
16. Purves, D., Lotto, R.B., and Nundy, S. (2002). Why we see what we do. American Scientist *90*, 236–243.
17. Naber, M., and Nakayama, K. (2013). Pupil responses to high-level image content. J Vision *13*, 7–7.
18. Fotiou, D.F., Brozou, C.G., Tsiptsios, D.J., Fotiou, A., Kabitsi, A., Nakou, M., Giantselidis, C., and Goula, A. (2007). Effect of age on pupillary light reflex: evaluation of pupil mobility for clinical practice and research. Electromyo Clin Neur *47*, 11–22.
19. Bergamin, O., and Kardon, R.H. (2003). Latency of the Pupil Light Reflex: Sample Rate, Stimulus Intensity, and Variation in Normal Subjects. Investigative Opthalmology Vis Sci *44*, 1546.
20. Ellis, C.J. (1981). The pupillary light reflex in normal subjects. Brit J Ophthalmol *65*, 754.
21. Young, M.J., and Lund, R.D. (1994). The anatomical substrates subserving the pupillary light reflex in rats: Origin of the consensual pupillary response. Neuroscience *62*, 481–496.
22. Clarke, R.J., and Ikeda, H. (1985). Luminance and darkness detectors in the olivary and posterior pretectal nuclei and their relationship to the pupillary light reflex in the rat. Exp Brain Res *57*, 224–232.
23. Gandhi, T., Kalia, A., Ganesh, S., and Sinha, P. (2015). Immediate susceptibility to visual illusions after sight onset. Curr Biol *25*, R358–R359.
24. Vasilev, D., Watanabe, M., Logothetis, N.K., and Totah, N.K. (2022). Focusing perceptual attention in one modality constrains subsequent learning in another modality. Biorxiv, 2022.01.22.477334.
25. Ho, J., Tumkaya, T., Aryal, S., Choi, H., and Claridge-Chang, A. (2019). Moving beyond P values: data analysis with estimation graphics. Nat Methods *16*, 565–566.
26. Calin-Jageman, R.J., and Cumming, G. (2019). Estimation for Better Inference in Neuroscience. Eneuro *6*, ENEURO.0205-19.2019.
27. Keysers, C., Gazzola, V., and Wagenmakers, E.-J. (2020). Using Bayes factor hypothesis testing in neuroscience to establish evidence of absence. Nat Neurosci *23*, 788–799.

Acknowledgements

We thank Claudius Kratochwil for comments on the manuscript. We wish to thank the Finnish Grid and Cloud Infrastructure (FGCI) for supporting this project with computational and data storage resources. This work was funded by the Max Planck Society and the University of Helsinki (Helsinki Institute of Life Science). This paper was typeset with the bioRxiv word template by @Chrelli: www.github.com/chrelli/bioRxiv-word-template

Author contributions

Conceptualization – NT; Data acquisition and curation – DV, IR; Formal analysis – DV, NT; Methodology – DV, NT; Project administration – NT; Supervision – NT; Visualization – NT; Writing – NT.

Competing interest statement

The authors have no competing interests to disclose.

Materials and Methods

Subjects

Male, Lister-Hooded rats (140 grams to 190 grams) were obtained from Charles River. After a 7-day acclimation period, rats were implanted with

a chamber and head-post and, in some cases, an EEG array. After implantation, rats were single housed. Experiments were carried out during the rats' active phase (housing illumination from 7PM to 7AM). All procedures were carried out with the prior approval of local authorities and in compliance with the European Community Guidelines for the Care and Use of Laboratory Animals.

Surgical procedures

The surgical procedure was identical to prior work [24]. Briefly, the rat was anesthetized using isoflurane and head-fixed using ear bars. We administered buprenorphine (0.06 mg/kg, s.c.), meloxicam (2.0 mg/kg, s.c.), enrofloxacin (10.0 mg/kg, s.c.), and lidocaine (0.5%, s.c. over skull) and waited 10 – 15 min (and for lack of response to paw pinch) before beginning surgical procedures. An EEG array (Neuronexus, CM32) was laid onto the cleaned and dried skull and fixed in place using dental cement (2-stage, powder/liquid Paladur). A custom-made skull implant was used for head-fixation (machine shop, Max Planck Institute for Biological Cybernetics). The implant was fixed onto the skull using UV-curing primer and dental cement (Tetric Evoflow, Dental Bauer). A craniotomy was made on the left occipital bone for a ground wire (99.9% pure silver). One end was flattened using an industrial press into a ~1-2 mm wide rectangle, which then was twisted into a roll to fit the craniotomy and inserted into the space between bone and dura. A rolled shape was used to increase the potential surface area in contact with CSF. The craniotomy was filled with viscous agar, which stabilized the wire and provided a conductive medium between the ground wire and the CSF. The other end of the ground wire was soldered to the ground wire of the electrode interface board of the EEG array. The wires and array were buried under dental cement (Paladur). The skin around the implant was glued to the implant using tissue glue (Histoacryl, B. Braun). Post surgical recovery lasted five days. During the first three days (surgery itself was counted as day one), the rat was injected either every 12 hours with buprenorphine or every 24 hours with meloxicam (same dosages as pre-operative). During the first five days, enrofloxacin was injected every 24 hours (same dosage as pre-operative). A rehydrating, nutritious, easily consumed, and palatable food was provided during recovery (DietGel Recovery, Clear H2O).

Handling and habituation

Rats were handled daily for at least five minutes per day from the day of arrival in housing until the day of surgery, which was 7 days. Animals were neither food nor water restricted. Habituation consisted of one session (~25 minutes) of head-fixation on a freely-rotating treadmill in front of a computer screen. Rats were free to run or remain immobile and a mixture of locomotor activity was observed.

Visual stimuli and stimulus presentation

Stimuli consisted of the Asahi stimulus, the control stimulus, and a grey screen used during the inter-stimulus interval. All stimuli were equiluminant (15 – 16 lux measured at the head-post). Stimuli were presented 50 cm from the rat's head. The resolution was 1280 pixels by 720 pixels. Stimuli were created in Adobe Illustrator with a canvas set to match the screen resolution. These files were exported to JPEG at 72 ppi. The stimuli were presented using Psychtoolbox implemented in MATLAB. The stimuli were presented at four visual angles (10º, 20º, 40º, and 60º) and in two colors (yellow, 580 nm, HEX: #ffff00 and green, 508 nm, HEX: #00ff28). As many stimuli were placed on the screen as possible, thus covering the entire visual field or most of it. Stimuli were presented for a duration of 4 sec. The inter-stimulus intervals were drawn from a distribution with a flat hazard rate that spanned 4 to 8 sec with a 0.5 sec resolution.

Pupillometry data acquisition and processing

Videos were recorded at 45 frames per second from the rat's right eye with near-infrared illumination (Thor Labs LED, M850L3 and Thor Labs Collimation optics, COP4-B). Frames were acquired using a near-infrared camera (Allied Vision, G-046B) and variable zoom lens, fixed 3.3x zoom lens, and 0.25x zoom lens attachment (Polytec, 1-60135, 1-62831, 6044). Acquisition occurred over a GigE connection (MATLAB image processing toolbox). The camera provided a TTL pulse with each video frame. These TTL pulses were recorded directly into the neurophysiology system (Neuralynx).

We used an in-house custom algorithm and computer code to extract pupil size from the recorded video frames. The procedure is reviewed in detail in prior work [24]. Briefly, images were Gaussian blurred, converted into a binary image, and then subjected to edge detection, closed contour detection, and fitting of ellipses to the closed contours. In cases where the algorithm was not able to find an ellipse of an area bigger than predefined minimal allowed area (or smaller than maximal, respectively), then the value of the pupil in this frame was left blank. This was also applied to the frames which captured the animal blinking. Blank frames were linearly interpolated. The pupil detection algorithm was implemented using the OpenCV package in Python 3.7.

The pupil size was normalized to a pre-stimulus baseline (1 sec duration) by calculating a z-score. The z-score was calculated on each trial by subtracting the baseline mean from each pupil size data point and then dividing this array by the standard deviation of the baseline data points. The latency for pupil constriction was calculated as in prior work [19]. We first smoothed the pupil size with an 11 point, 2nd order Savitzky-Golay filter (sgolayfilt in MATLAB). The signal was differentiated to obtain velocity and the velocity was lowpass filtered at 6 Hz with a 2nd order Butterworth filter (filtfilt in MATLAB). This signal was then differentiated to obtain acceleration and the latency to constrict was defined as the time point with the largest negative acceleration.

EEG signal acquisition and analysis

EEG signals were recorded using a flexible polyimide array with 32 platinum electrodes (Neuronexus, H32). Signals were recorded against animal ground, pre-amplified at the rat's head (Neuralynx, HS-36), and then amplified and digitized at 32 kHz (Neuralynx, Digital Lynx SX). The analysis focused on bilateral electrodes placed over frontal cortex (locations relative to Bregma: 1.5 mm anterior, ±1.2 mm lateral; 3.6 mm anterior, ±1.2 mm lateral) and visual cortex (locations relative to Bregma: 5.0 mm posterior, ±1.5 mm lateral; 5.0 mm posterior, ±3.0 mm lateral; 5.0 mm posterior, ±4.4 mm lateral; 7.0 mm posterior, ±1.5 mm lateral; 7.0 mm posterior, ±3.0 mm lateral; 7.0 mm posterior, ±4.4 mm lateral). EEG signals were first low pass filtered at 5 Hz and then downsampled to 320 Hz. The entire signal was mean subtracted. EEG topographical plots were produced using the MATLAB command, scatteredInterpolant with natural neighbor interpolation. The contour plots (contourf function in MATLAB) used 50 levels.

Statistics

We used estimation statistics and report effect sizes and the confidence intervals for effect sizes (DABEST toolbox in MATLAB [25,26]). Bayesian statistics were used for assessing evidence (or lack thereof) for the null hypothesis and for the alternative hypothesis [27]. Bayesian statistics were calculated in JASP software.

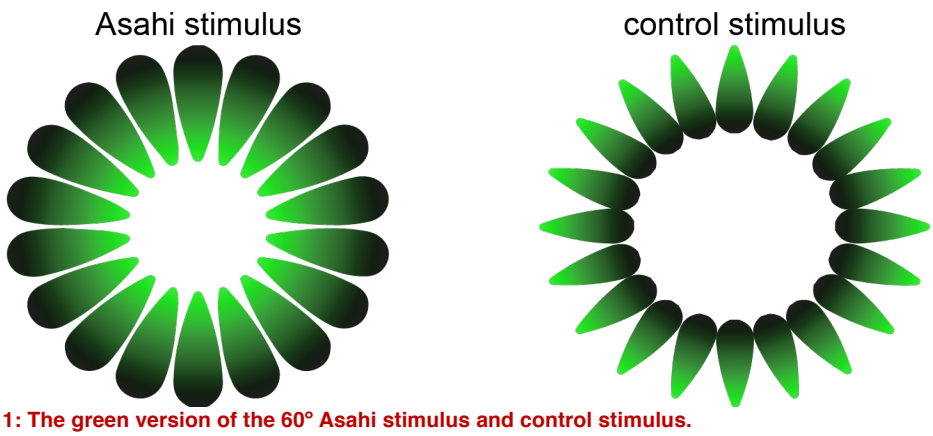

Supplementary Figure 1: The green version of the 60° Asahi stimulus and control stimulus.

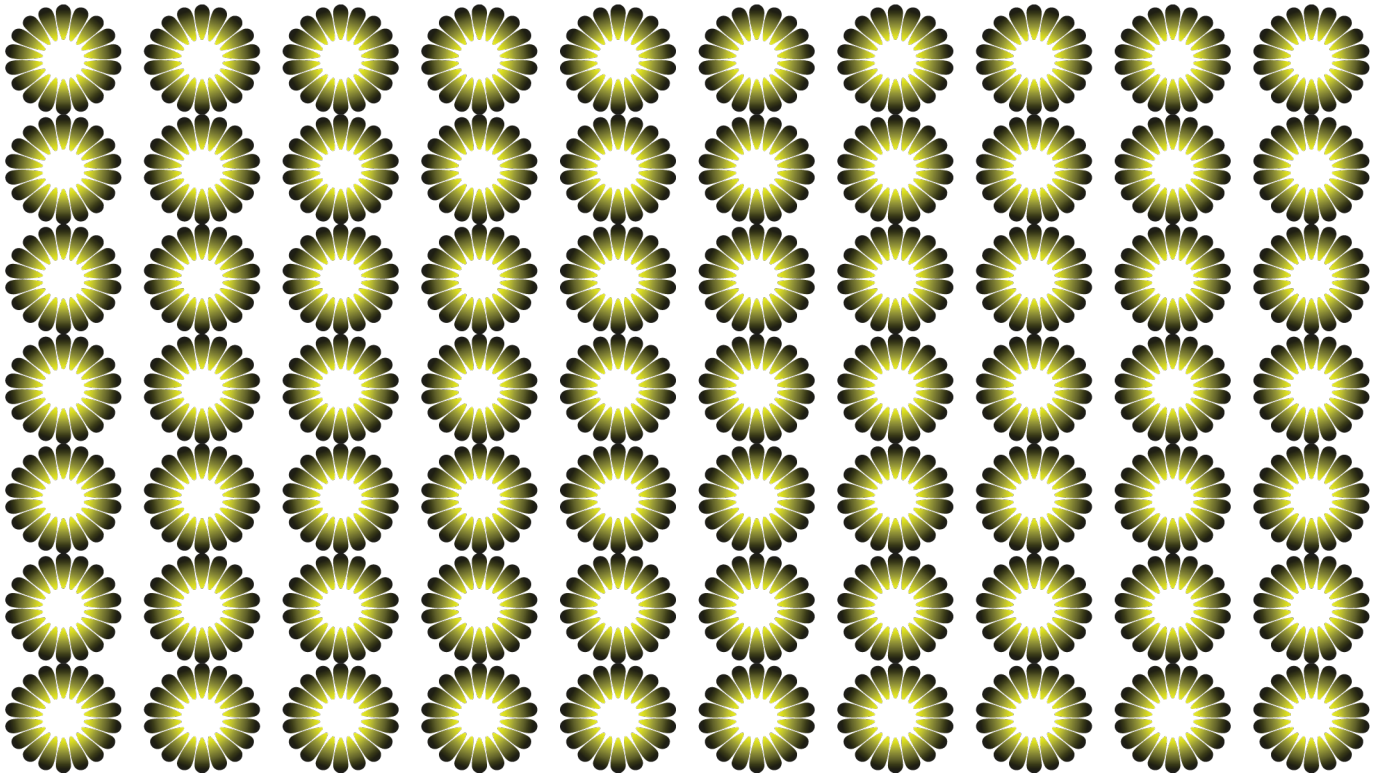

Supplementary Figure 2: The yellow version of the 10° Asahi stimulus.

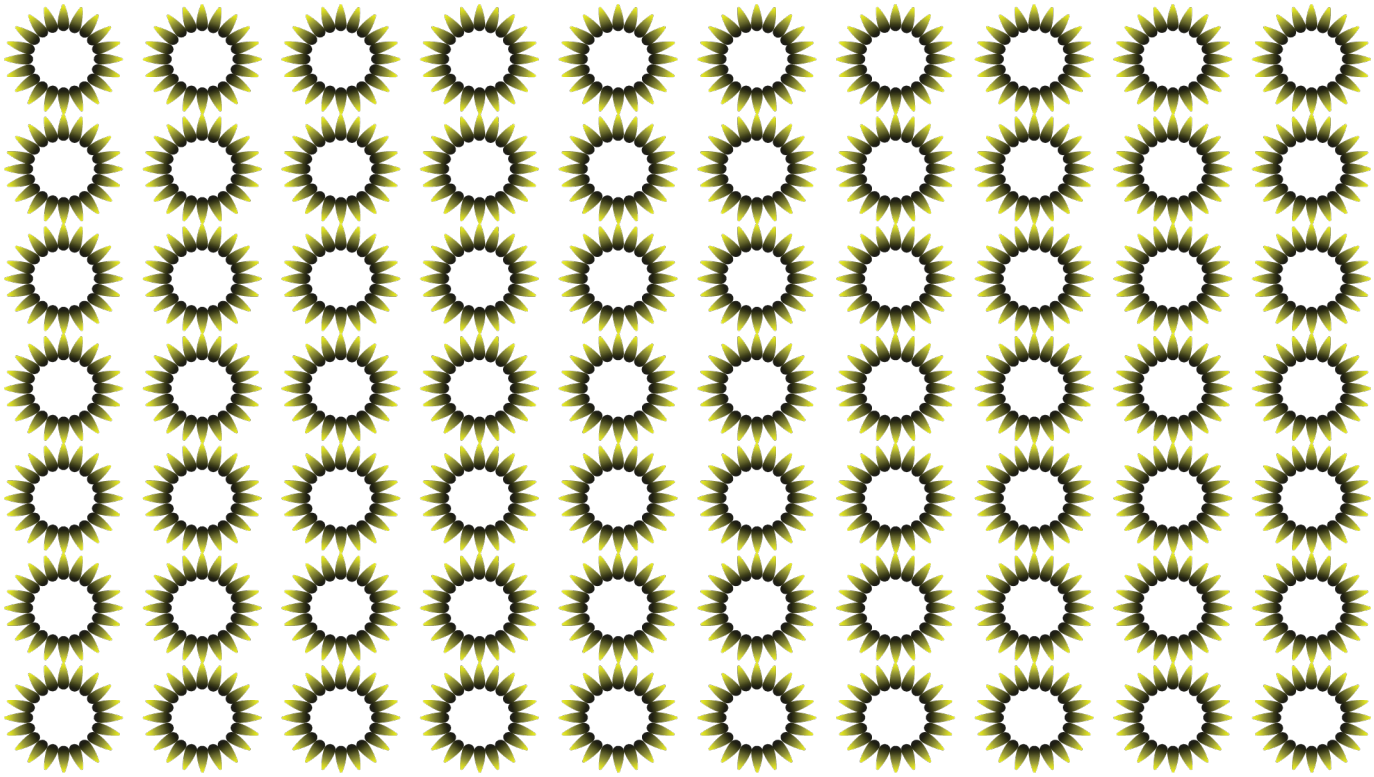

Supplementary Figure 3: The yellow version of the 10° control stimulus.

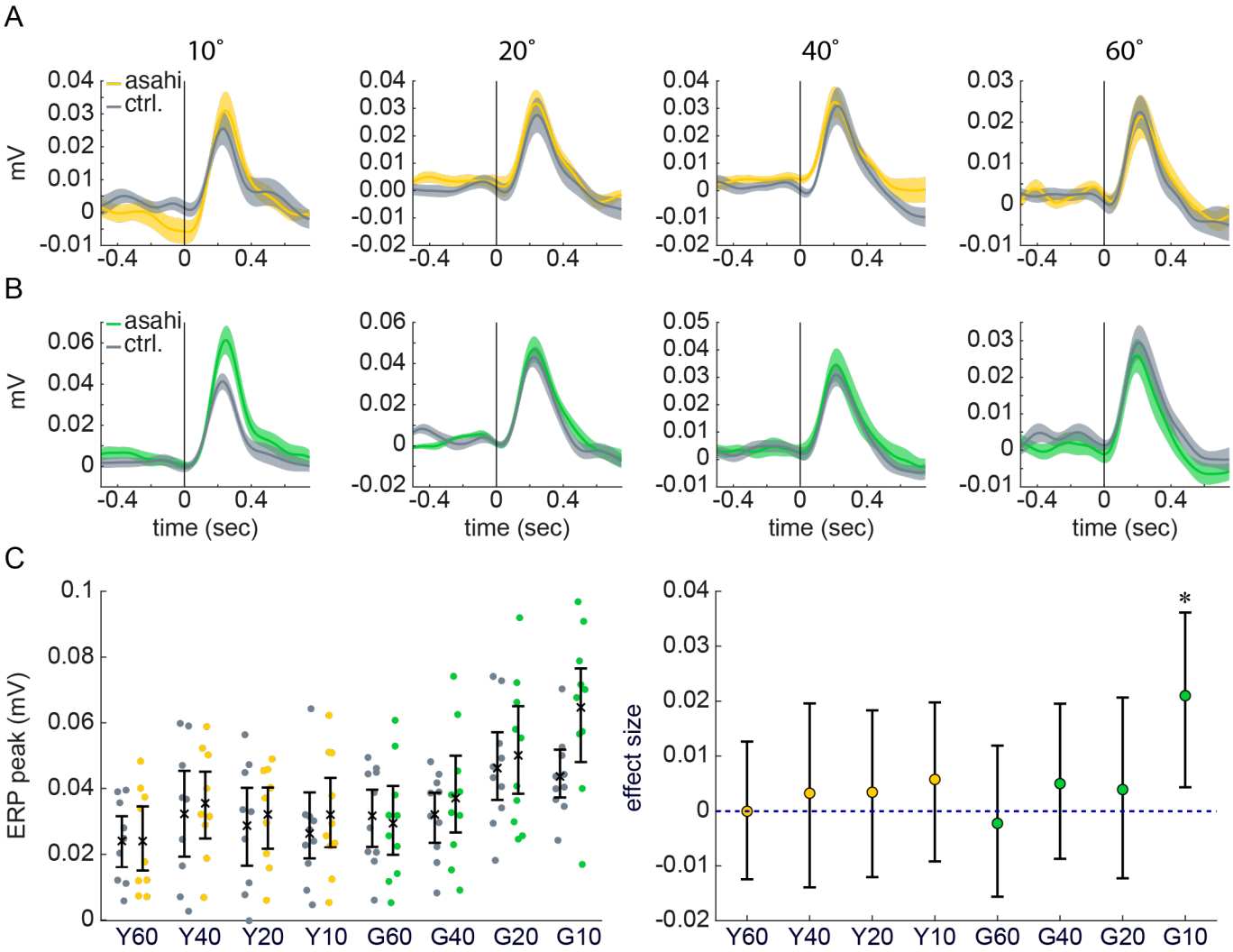

Supplementary Figure 4: The ERP after each stimulus. (A, B) The SEM of the visual cortex EEG is plotted from 750 msec before and until 750 msec after stimulus onset. The grey line is the ERP around the control stimulus and the colored line is relative to the Asahi stimulus. Panel A shows the ERP to yellow stimuli and panel B shows the ERP to green stimuli. (C) The maximal potential in the ERP is plotted for each stimulus. Dots are individual rats. Note that one of the ten rats was not recorded in the yellow stimuli condition. The right panel shows the effect size between the Asahi stimulus and the control stimulus. The asterisk indicates support for the alternative hypothesis (BF10 > 3).